15th International Conference on Fluid Control, Measurements and Visualization
27-30 May, 2019, Naples, Italy

Modeling and Hysteresis Compensation Using Asymmetric Bouc-Wen Model for Tap-water Driven Muscle and Its Application to Adaptive Model Predictive Tracking Control

Ryo Inada[1,*], Kazuhisa Ito[2], Shigeru Ikeo[3]

[1]Graduate School of Mechanical Engineering, Shibaura Institute of Technology, Saitama, Japan
[2]Department of Machinery and Control Systems, Shibaura Institute of Technology, Saitama, Japan
[3]Department of Engineering and Applied Sciences, Sophia University, Chiyoda-ku, Japan
[*]md18012@shibaura-it.ac.jp

Abstract This paper is concerned with modeling, linearization technique, and displacement control strategies of tap water driven muscle. Recently, industrial applications of McKibben type artificial muscle has been a significant increase because it has advantages such as high flexibility, low cost, light weight, and high-power density. In particular, tap water driven muscle possesses advantages of water hydraulic system and the muscle is promising to apply to industrial machines that require high cleanliness. However, the muscle has strong asymmetric hysteresis characteristics which are changed by a load applied to the muscle. Therefore, it is difficult to construct a precise muscle model and to achieve higher displacement control. For these problems, this paper proposes a muscle model that consists of a linear model and an asymmetric Bouc-Wen model, which enables a description of asymmetric hysteresis characteristics having relatively simple structure. Constrained recursive least square (RLS) algorithm then estimates parameters of the proposed model and inverse of the model is used as linearization technique. In order to improve control performance, the authors employ model predictive control (MPC) with servo mechanism based on obtained model. Moreover, adaptive mechanism is introduced (hereafter, AMPC) to enhance robustness for change of load and reference. Comparing these approaches, experimental results showed that AMPC with servo mechanism using linearization technique can improve control performance under different load conditions and references.
Keywords: McKibben type artificial muscle, Tap water hydraulics, Model predictive tracking control, Constrained recursive least square, Asymmetric Bouc-Wen model

1 Introduction

McKibben type artificial muscle is an outstanding actuator and has been applied to biorobotic, medical, and industrial applications because it exhibits advantages including high flexibility, low cost, light weight, and high-power density [1]. On the other hand, tap water driven systems, which use pure tap water as working fluid, have advantages such as no risks of environmental pollution, easily disposable, readily available, and requiring no power source [2][3]. Given the aforementioned aspects, McKibben type artificial muscle driven by tap water (hereafter, tap water driven muscle) is promising to apply to mechanical systems that require high cleanliness or support systems at home because the muscle has advantages of tap water driven and McKibben type artificial muscle. However, the muscle has strong asymmetric hysteresis characteristics caused by nonlinear contraction behavior and friction between components. In addition, its characteristics depend on load applied to the muscle. Therefore, it is difficult to derive a model expressing its behavior and to design controller for high-performance displacement control. Most of previous studies already propose robust or adaptive scheme such as the model reference adaptive control [4], sliding mode control [5], and H_∞ control [6] in order to solve the aforementioned problems. Nevertheless, the control methods are designed based only on a linear model. Linearized models potentially limit the operation point and control performance because the models ignore the effects of nonlinear hysteresis. Therefore, control systems based only on the linear model of the artificial muscles cannot achieve precise control. Furthermore, nonlinear control strategies are also used for displacement control of the muscle [7][8]. However, in order to express nonlinearities, the control methods have a complex structure and require information on the estimated objects and prior measurements to identify parameters of the model due to the control methods designed based on the first-principles-model. Therefore, the nonlinear control strategies are not suitable for application.

In previous studies, some conventional nonlinear hysteresis models including Prandtl-Ishlinskii, Preisach or Bouc-Wen model have been applied to the muscle [9]-[11]. These hysteresis models can express hysteresis characteristics and do not need measure physical parameters. In particular, the Bouc-Wen model is the most suitable for control of the other hysteresis models because this model has a relatively simple linear structure when compared to those. Control system based on this model shows that control performance is improved when compared to control systems based only on the linear model. However, its control system cannot achieve high precision displacement control because, generally, Bouc-Wen model cannot express asymmetric hysteresis characteristics. Therefore, to improve high control performance, a model that compensates such hysteresis characteristics of the muscle and a control system based on its model are required.

In this study, the authors derive a model of tap-water driven muscle system using an asymmetric Bouc-Wen model that is combined standard Bouc-Wen model with a polynomial function of displacement of the muscle and estimate parameters of the model by recursive least squares (RLS) algorithm, which is an adaptive identification with robustness for measurement noise. The asymmetric Bouc-Wen model has already been applied to a piezoelectric actuator, although the model has not ever been applied to the muscle including not only the tap water driven muscle but also a pneumatic artificial muscle. The authors observe effectiveness of the asymmetric Bouc-Wen model for the muscle [12]. Then, we apply model predictive control (MPC) with linearization technique using inverse of proposed model that consists of a linear model and the asymmetric Bouc-Wen model for performance improvement. The MPC corresponds to optimal control and generates a control input to optimize an evaluation function including a predicted state/output and input over a given finite future horizon with constraints (for *e.g.*, input and state) at every control steps. Given the aforementioned aspects, the MPC is widely used in various field such as aerospace and automotive industries[13] and is a very promising control method. The control method depends significantly on precision of a mathematical model because the MPC utilizes it to predict a future behavior. Therefore, we implement the proposed model combining the linear model with the asymmetric Bouc-Wen model to obtain high control performance. However, it is not possible to apply the MPC with multi coincidence points to the muscle system in a straightforward manner with a popular MPC solver, such as CVXGEN, which generates the code to solve a convex programming problem [14] because the model contains nonlinearities. In order to apply this solver, this paper proposes a linearization technique for the muscle system by designing a proper input that compensates the effect of hysteresis characteristics by using the inverse of the asymmetric Bouc-Wen model.

Additionally, to obtain high tracking performance, MPC with servo mechanism, whose evaluation function is augmeted to include a discrete integrator, is introduced. Furthermore, this study introduces an adaptive model predictive control (AMPC) that incorporate the MPC into RLS algorithm in order to compensate parameters changing of the muscle when the load applied to the muscle is changed. However, in terms of application, the generated control input may diverge if a few estimated parameters corresponding to the effect of hysteresis converge to an extremely small value. Therefore, this study introduces constrained RLS algorithm to AMPC based on preliminary identification to constrain the parameters estimation within a certain region. In order to demonstrate the effectiveness of the AMPC with the servo mechanism, experiments are conducted and the results are compared to the unique coincidence point AMPC that directly uses the model under two different load conditions and references.

Nomenclature

β, γ	Hysteresis parameters that determine the shape of the hysteresis
$\Delta u(k)$	Change of valve input voltage
$\Delta u_c(k)$	Change of control input by MPC with the servo mechanism
$\hat{\theta}(k)$	Estimated parameter vector
$\hat{l}(k)$	Free response
$\hat{l}(k)$	Output of the model
$\phi(k)$	Regressor vector
θ	Parameter space
θ_0	Initial value of the estimated parameter vector
A_i	Hysteresis parameter that determines an amplitude
a_i, b_i	System parameters
C	Constrained region in the parameter space
$g(\cdot)$	Polynomial function
H_p	Prediction horizon
H_u	Control horizon
$l(k)$	Displacement of the muscle
n	Hysteresis parameter that determines smoothness
$P(k)$	Covariance matrix
Q	Weight on the tracking error
Q_s	Weight on the integrator
R	Weight on change of input
$r(k)$	Reference trajectory
$S(H_p)$	Step response
$u(k)$	Valve input voltage
$u_c(k)$	Control input by MPC with the servo mechanism
$y_{hy}(k)$	Virtual hysteresis variable

2 Modeling of tap water driven muscle and estimation of its parameter

2.1 Modeling of tap water driven muscle using asymmetric Bouc-Wen model

Several asymmetric Bouc-Wen models are already proposed for describing hysteresis of a plant. In this study, we adopt asymmetric Bouc-Wen model proposed in [12] for simple structure. However, that asymmetric Bouc-wen model is represented via differential equations and MPC approach cannot directly be applicable. Therefore, the asymmetric Bouc-Wen model is disretized by applying forward difference approximation. In this study, Eq.(1) which gives better fitness in preliminary identification was introduced. Eq.(1) shows the muscle model that combines a linear model with the discretized asymmetric Bouc-Wen model

$$\begin{cases} l(k) = a_1 l(k-1) + a_2 l(k-2) + b_1 u(k-1) + y_{hy}(k-1) + y_{hy}(k-2) \\ y_{hy}(k-i) = A_i\{l(k-i) - l(k-1-i)\} - \beta_i |l(k-i) - l(k-1-i)| y_{hy}(k-1-i) \\ \qquad\qquad - \gamma_i \{l(k-i) - l(k-1-i)\} |y_{hy}(k-1-i)| + c_i y_{hy}(k-1-i) + g(l(k-i)) \\ g(l(k-i)) = \sum_{j=2}^{n} \xi_{ij} l^j(k-i) \end{cases} \tag{1}$$

where k denotes time step and $i = 1, 2$. Note that the proposed model possesses not only the muscle's dynamics but also proportional valve's dynamics. The proposed model incorporates the linear model corresponding from the first term to the third term and the asymmetric Bouc-Wen model with the fifth and sixth terms. Here, a standard Bouc-Wen model is expressd as Eq.(1) without $g(l(k))$ which is the polynomial function of displacement of the muscle. The model (1) can express asymmetric hysteresis by choosing $g(l(k))$ as odd function.

2.2 Linearization technique using the proposed model

The authors propose linearization technique for the proposed model to apply code generator, *e.g.* CVXGEN, which quickly solves the convex programming problem with linear constraints.

The linearized plant is defined as follows:

$$l(k) = a_1 l(k-1) + a_2 l(k-2) + b_1 u_c(k-1) \tag{2}$$

where $u_c(k)$ is to be designed in Section 3.2. By substituting Eq.(2) into Eq.(1), we obtain the following hysteresis cancellation input:

$$u(k) = u_c(k) - \frac{1}{b_1}(y_{hy}(k) + y_{hy}(k-1)) \tag{3}$$

By inputting Eq.(3), the system is linearized and we can apply CVXGEN to the muscle system.

2.3 Constrained RLS algorithm for the proposed model

Recursive least square algorithm corresponds to on-line identification algorithm and the parameter updating law for RLS algorithm [15] is expressed as follows:

$$\begin{cases} \hat{\theta}(k) = \hat{\theta}(k-1) + \dfrac{P(k-1)\phi(k-1)}{1+\phi^T(k-1)P(k-1)\phi(k-1)}\{l(k) - \phi^T(k-1)\hat{\theta}(k-1)\} \\ P(k-1) = P(k-2) - \dfrac{P(k-2)\phi(k-1)\phi^T(k-1)P(k-2)}{1+\phi^T(k-1)P(k-2)\phi(k-1)} \end{cases} \tag{4}$$

where $\phi(k)$ and $\hat{\theta}(k)$ are defined as follows:

$$\phi(k-1) = \begin{bmatrix} l(k-1) \\ l(k-2) \\ u(k-1) \\ l(k-1)-l(k-2) \\ l(k-2)-l(k-3) \\ |l(k-1)-l(k-2)|y_{hy}(k-2) \\ |l(k-2)-l(k-3)|y_{hy}(k-3) \\ \{l(k-1)-l(k-2)\}|y_{hy}(k-2)| \\ \{l(k-2)-l(k-3)\}|y_{hy}(k-3)| \\ y_{hy}(k-2) \\ y_{hy}(k-3) \\ l^2(k-1) \\ l^2(k-2) \\ l^3(k-1) \\ l^3(k-2) \end{bmatrix}, \quad \hat{\theta}(k) = \begin{bmatrix} a_1(k) \\ a_2(k) \\ b_1(k) \\ A_1(k) \\ A_2(k) \\ \beta_1(k) \\ \beta_2(k) \\ \gamma_1(k) \\ \gamma_2(k) \\ c_1(k) \\ c_2(k) \\ \xi_{21}(k) \\ \xi_{22}(k) \\ \xi_{31}(k) \\ \xi_{32}(k) \end{bmatrix}$$

where $n = 1$ in Eq.(1) and the order of $g(l(k))$ is 3. In particular, we conduct parameter estimation assuming that $y_{hy}(k)$ is the difference between displacement of the muscle and output of linear model, namely $y_{hy}(k) = l(k) - [a_1 l(k-1) + a_2 l(k-2) + b_1 u(k-1)]$ because $y_{hy}(k)$ cannot be measured due to virtual variable [16] .

Here, b_1 in hysteresis cancellation input (3) is unknown. b_1 should be replaced with $\hat{b}_1(k)$ which is an estimated parameter of b_1 at time k as

$$u(k) = u_c(k) - \frac{1}{\hat{b}_1(k)}(y_{hy}(k) + y_{hy}(k-1)) \tag{5}$$

to deal with hysteresis cancellation input. For application, we have to constrain parameter region to ensure that $\hat{b}_1(k)$ does not converge to around zero because the generated control input (5) may diverge if $\hat{b}_1(k)$ in denominator of hysteresis cancellation input converges to an extremely small value. Therefore, it is necessary to introduce constrained RLS algorithm. Constrained RLS algorithm is run by the following algorithm [15].

Algorithm 1 Constrained RLS

Step 1: Set $k = 0$, $\hat{\theta}(0)$, $P(-1)$.

Step 2: Measure the elements of $\phi(k)$.

Step 3: Calculate Eq.(4).

if $\hat{\theta}(k) \in C$ **then**

Utilize it as estimated parameter at time k.

else

Transform the coordinate basis for the parameter sapce by defining the following

$\rho = P^{-1/2}(k-1)\theta$

and denote $\bar{C}$ as the image of C under linear transformation $P^{-1/2}(k-1)$.

Orthogonally project the image, $\hat{\rho}(k)$, of $\hat{\theta}(k)$ under $P^{-1/2}(k-1)$ onto the boundary of $\bar{C}$ to yield $\hat{\rho}'(k)$ where the following expression holds:

$\hat{\rho}(k) = P^{-1/2}(k-1)\hat{\theta}(k)$

Put

$\hat{\theta}(k) = \hat{\theta}'(k) = P^{1/2}(k-1)\hat{\rho}'(k)$

and utilize it as estimated parameter at time k.

end if

Step 4: set $k \leftarrow k+1$ and go to **Step 2**.

Remark 1. The transformation $\rho = P^{-1/2}(k-1)\theta$ yields the following:

$$V(k) = \left[\hat{\theta}(k) - \theta_0\right]^T P^{-1}(k-1)\left[\hat{\theta}(k) - \theta_0\right] \tag{6}$$

$$= \left[\hat{\rho}(k) - \rho_0\right]^T \left[\hat{\rho}(k) - \rho_0\right] \tag{7}$$

where

$$\rho_0 = P^{-1/2}(k-1)\theta_0 \in \bar{C} \tag{8}$$

Given that $\hat{\rho}'(k)$ is an orthogonal projection of $\hat{\rho}(k)$ on $\bar{C}$ and $\rho_0 \in \bar{C}$, the following inequality holds:

$$\|\hat{\rho}'(k) - \rho_0\|^2 \leq \|\hat{\rho}(k) - \rho_0\|^2 \tag{9}$$

and hence

$$\left[\hat{\theta}'(k) - \theta_0\right]^T P^{-1}(k-1)\left[\hat{\theta}'(k) - \theta_0\right] \leq \left[\hat{\theta}(k) - \theta_0\right]^T P^{-1}(k-1)\left[\hat{\theta}(k) - \theta_0\right] \tag{10}$$

From the result, we observe that $\left[\hat{\theta}(k) - \theta_0\right]^T P(k-1)^{-1}\left[\hat{\theta}(k) - \theta_0\right]$corresponds to a non-increasing function when $\hat{\theta}(k)$ is projected on the constrained region C.

2.4 Experimental circuit and setup

Figures 1 and 2 show experimental circuit and setup, respectively. Table 1 shows circuit components.

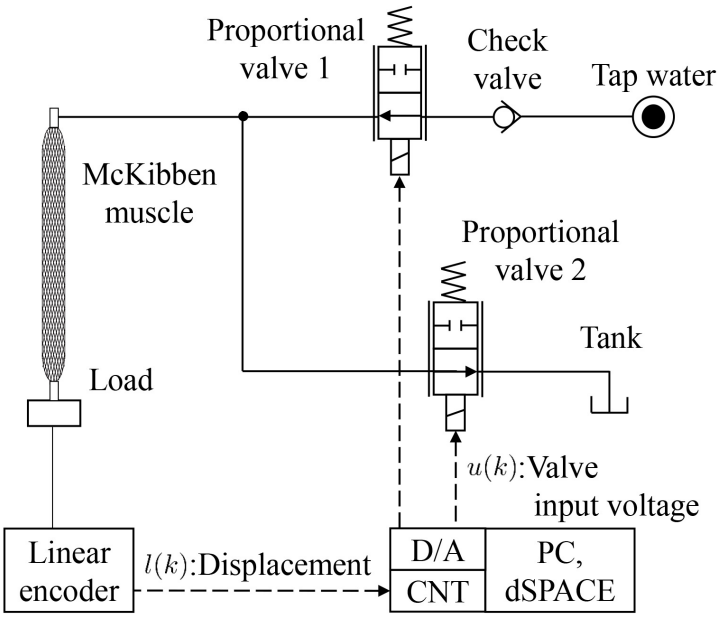

Fig. 1 Experimental circuit

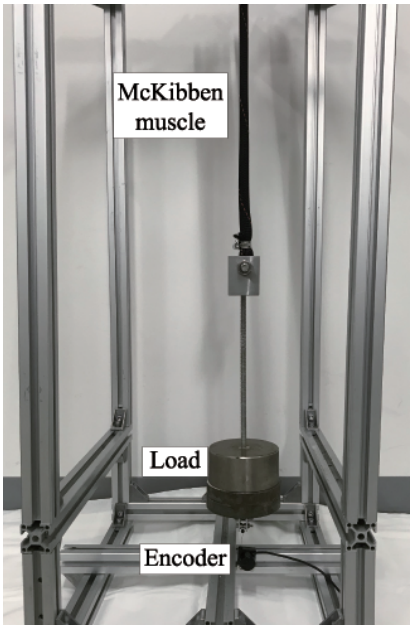

Fig. 2 Experimental setup

Table 1 Components of experimental circuit

Item	Specifications
Proportional valves	KFPV300-2-80, Koganei Corporation Cv Value: 1.6, Range of input voltage: 0 to 10 [V]
Pressure sensor	FP101, Yokogawa Electric Corporation Range: 0 to 1 [MPa(G)]
Linear encoder	DX-025, MUTOH Industries Ltd. Resolution: 0.01 [mm]
PC	Windows 7, Microsoft Corporation CPU: 3.10 [GHz], RAM: 4.00 [GB] Including MATLAB/Simulink and dSPACE 1103
Tap water driven muscle	In-house custom-built muscle Length: 400 [mm]
Tap water	Average supply pressure: 0.25 [MPa(G)]

We conduct parameter estimation for the proposed model that consists of linear model and the asymmetric Bouc-Wen model and conventional model that consists of linear model and standard Bouc-Wen model by using constrained RLS algorithm. Note that standard Bouc-Wen model indicates Eq.(1) without $g(l(k))$. Figure 3 shows a part of the input corresponding to valve input voltage and output corresponding to displacement of the muscle using parameter estimation. As seen in the figure, a sinusoidal wave with an amplitude of 3 [V], bias

of 5 [V], and frequency of 0.1 [Hz] is given. In addition, the sampling period is 0.1[s] and the load applied to the muscle corresponds to 44 [N]. The initial value of the covariance matrix $P(-1)$ corresponds to a diagonal matrix with a value of 10^3 for each element, and the initial estimated parameter vector $\hat{\theta}(0)$ corresponds to zero. Table 2 summarizes the constrained region of the parameters of the linear model in Eq.(1) that are obtained via preliminary system identification experiments and the region is determined via the mean value and distribution of each parameter.

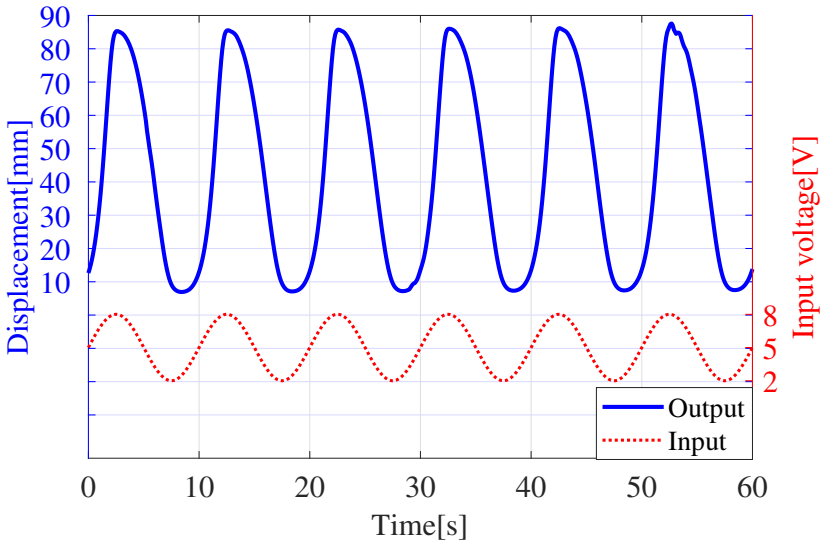

Fig. 3 Part of input (valve input voltage) and output (displacement of muscle) data for identification

Table 2 Constrained region of linear model in Eq.(1) obtained by preliminary system identification experiments

	a_1	a_2	b_1
Minimum value	1.208	-0.334	0.607
Maximum value	1.260	-0.278	1.184

Table 3 summarizes estimated parameters of the proposed model and conventional model. It is estimated that the parameters almost converge in approximately 120 [s] although constrained RLS algorithm runs after 120 [s]. Figure 4 shows a comparison of the proposed model and the conventional model respectively by substituting the estimated parameters shown in Table 3 into Eq.(1). As Fig.4 shows, it is evident that the conventional model does not sufficiently express the measured displacement of the muscle while proposed model gives close agreement with that. In addition, Fig.5 demonstrates comparison of hysteresis loop of the proposed model and conventional model. From this Figure, we observe that the conventional model using standard Bouc-Wen model does not compensate the asymmetric hysteresis loop while the proposed model using the asymmetric Bouc-Wen model expresses the asymmetric hysteresis. Table 4 shows fitness between predicted output of the model and experimental measurement data. As shown in the Table, proposed model maintains that fitness between predicted output of the proposed model and experimental measurement data is higher than 90 [%] over the simulated output. The results clarifies that proposed model that combines the linear model the asymmetric Bouc-Wen model is valid for asymmetric hysteresis characteristics of the muscle and constrained RLS algorithm appropriately estimates parameters of the proposed model.

Table 3 Parameters of the proposed model and conventional model as estimated by RLS algorithm

Parameter	Value	
	Proposed model (asymmetric Bouc-Wen model	Conventional model (standard Bouc-Wen model)
a_1	1.260	1.260
a_2	−0.288	−0.304
b_1	0.607	0.607
A_1	0.174	0.222
A_2	0.145	−0.088
β_1	−0.023	−0.684
β_2	−0.027	0.333
γ_1	−0.152	0.387
γ_2	0.169	−0.098
c_1	0.082	0.290
c_2	0.049	0.156
ξ_{21}	0.003	-
ξ_{22}	−0.003	-
ξ_{31}	-6.413×10^{-5}	-
ξ_{32}	-5.568×10^{-5}	-

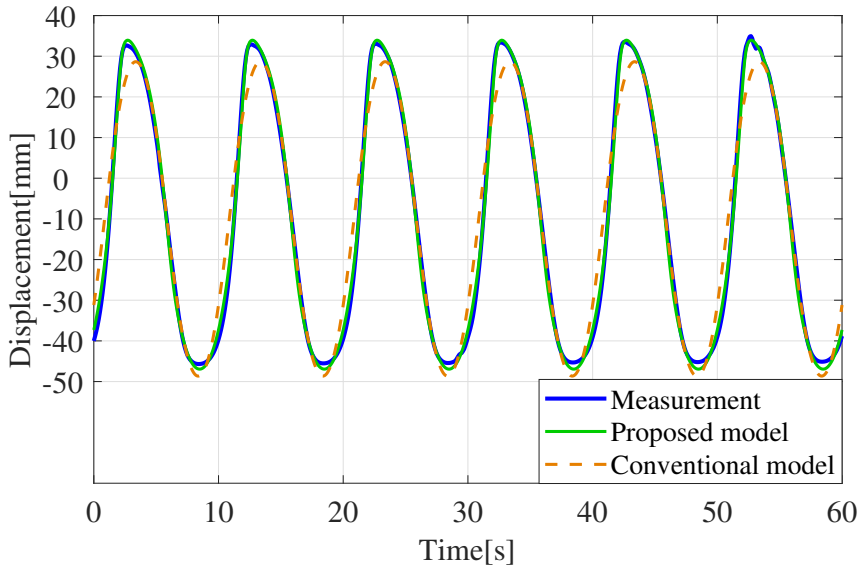

Fig. 4 Comparison of the proposed model and conventional model in the experiment

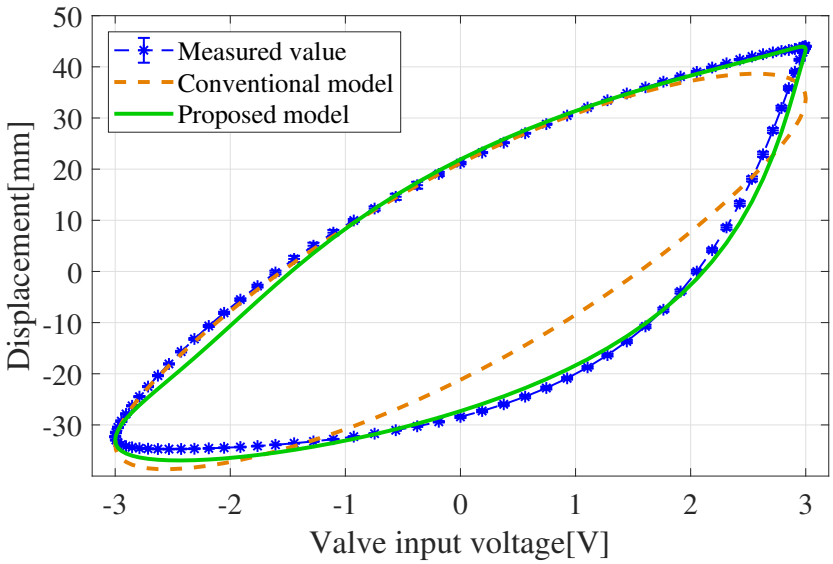

Fig. 5 Comparison of hysteresis loop of proposed model and conventional model for 0.1 [Hz] sinusoidal valve input voltage in the experiment

Table 4 Control parameters of each control method for the displacement control

Model \ Prediction	1-step ahead	3-step ahead	5-step ahead	Simulated output
Proposed model	99.6 [%]	98.3 [%]	96.8 [%]	93.6 [%]
Conventional model	99.5 [%]	97.4 [%]	93.9 [%]	81.9 [%]

3 Controller design for MPC

3.1 MPC with unique coincidence point

Model predictive control generates optimal input to make the predicted output coincide with reference trajectory at $k, k+1, \ldots, k+H_p$ steps. Unique solution can be obtained by taking $H_p = H_u$. In particular, MPC with unique coincidence point is simplest case and only has unique coincidence point at time $k+H_P$. Additionally, this control method can directly deal with nonlinear model because the control method derives unique solution and does not require evaluation function. In this control method, designers firstly select a prediction horizon H_p and then reference trajectory $r(k)$ that adequately defines an output track reference from current output $l(k)$ to H_p steps ahead of the predicted output $\hat{l}(k+H_p|k)$ that is uniquely calculated by Eq.(11) as follows:

$$\hat{l}(k+H_p|k) = \hat{l}_f(k+H_p|k) + S(H_p)\Delta\hat{u}(k) \tag{11}$$

where $(k_1|k_2)$ denotes predicted value at step k_1 by calculating at step k_2. Additionally, free response $\hat{l}(k+H_p|k)$ and step response $S(H_p)$ indicate that is obtained at the coincidence point when least input $u(k-1)$ is maintained during H_p steps and unit step response of the model at H_p step later, respectively. In addition, the change of input is defined as follows:

$$\Delta u(k) = u(k) - u(k-1) \tag{12}$$

Note that the control method assumes that the optimal input $u(k)$ will only change at times k, and will remain constant after that. Finally, the controller generates optimal change of input that causes the predicted output

to coincide with the reference trajectory at $k+H_p$ steps, namely $r(k+H_p|k) = \hat{l}(k+H_p|k)$. Thus, the optimal change of input $u(k)$ is obtained as follows:

$$\Delta u(k) = \frac{r(k+H_p|k) - \hat{l}_f(k+H_p|k)}{S(H_p)} \tag{13}$$

From the result, we obtain a unique solution even when the nonlinear model is adopted. Here, valve input voltage $u(k)$ is calculated by Eq.(14) :

$$u(k) = \frac{1}{1-z^{-1}}\Delta u(k) \tag{14}$$

The algorithm iterates at each step.

3.2 MPC with servo mechanism

Model predictive control with a unique coincidence point was introduced in the previous section. In order to improve control performance, we introduce MPC with multi coincidence points to achieve a higher control performance. In general, MPC cannot generate optimal control input to make predicted output completely coincide with reference trajectory at each step. Therefore, in MPC with multi coincidence points, the evaluation function is introduced and control input corresponds to an optimizer of that function. The evaluation function of MPC with the servo mechanism [17] is described as follows:

$$J(k) = \sum_{i=1}^{H_p} |\hat{l}(k+i|k) - r(k+i|k)|^2_{Q(i)} + \sum_{i=0}^{H_u-1} |\Delta\hat{u}_c(k+i|k)|^2_{R(i)} + \sum_{i=1}^{H_p} |x_s(k+i|k)|^2_{Q_c(i)} \tag{15}$$

where $\Delta\hat{u}_c(k+i|k)$ is defined as Eq.(16)

$$\Delta\hat{u}_c(k+i|k) = \hat{u}_c(k+i|k) - \hat{u}_c(k+i-1|k) \tag{16}$$

The model derived by system identification or estimation generally does not possess a physical interpretation of the state vector. Therefore, a non-minimum state space representation is introduced as follows:

$$\begin{cases} \mathbf{x}(k+1) = A\mathbf{x}(k) + Bu(k) \\ \quad l(k) = C\mathbf{x}(k) \end{cases} \tag{17}$$

where A, B, C, and $\mathbf{x}(k)$ are defined as:

$$A = \begin{bmatrix} a_1 & a_2 \\ 1 & 0 \end{bmatrix},\ B = \begin{bmatrix} b_1 \\ 0 \end{bmatrix},\ C = \begin{bmatrix} 1 & 0 \end{bmatrix},\ \mathbf{x}(k) = \begin{bmatrix} l(k) \\ l(k-1) \end{bmatrix}$$

Discrete time integrator $x_s(k)$ is expressed as follows:

$$x_s(k+1) = x_s(k) + \{r(k) - l(k)\} \tag{18}$$

Here, we provide the input constraint of input voltage of control valves that is represented by Eq.(19) and $\Delta u_c(k)$ is derived by minimizing Eq.(15) subject to Eq.(19) as follows:

$$0 \le \hat{u}_c(k+i|k) - \frac{1}{\hat{b}_1(k)}(y_{hy}(k) + y_{hy}(k-1)) \le 10, i = 0, 1, \cdots, H_u - 1 \tag{19}$$

Here, valve input voltage $u(k)$ is obtained by substituting control input $u_c(k)$ calculated by Eq.(20) into Eq.(5).

$$u_c(k) = \frac{1}{1-z^{-1}}\Delta u_c(k) \tag{20}$$

The algorithm above iterates at each step.

3.3 Adaptive MPC with servo mechanism

Model predictive control utilizes the mathematical model to compute future response. Therefore, it is obvious that if the predictor has parameter error and/or parameters of the muscle are changed by the load, then MPC does not work well and control performance is degraded. In order to solve the problem, we incorporate constrained RLS algorithm into the predictor of MPC to compensate modeling error. Figures 6 and 7 show the schematic block diagram of adaptive model predictive control (AMPC) which combines MPC with constrained RLS algorithm with the servo mechanism using the hysteresis cancellation input and AMPC with unique coincidence point. Note that MPC/AMPC with servo mechanism utilize proposed model as linearization technique and their predictors are linear model expressed Eq.(2). In addition, MPC/AMPC with unique coincidence point directly utilize proposed model as predictor and does not use linearization technique as shown in Fig.7.

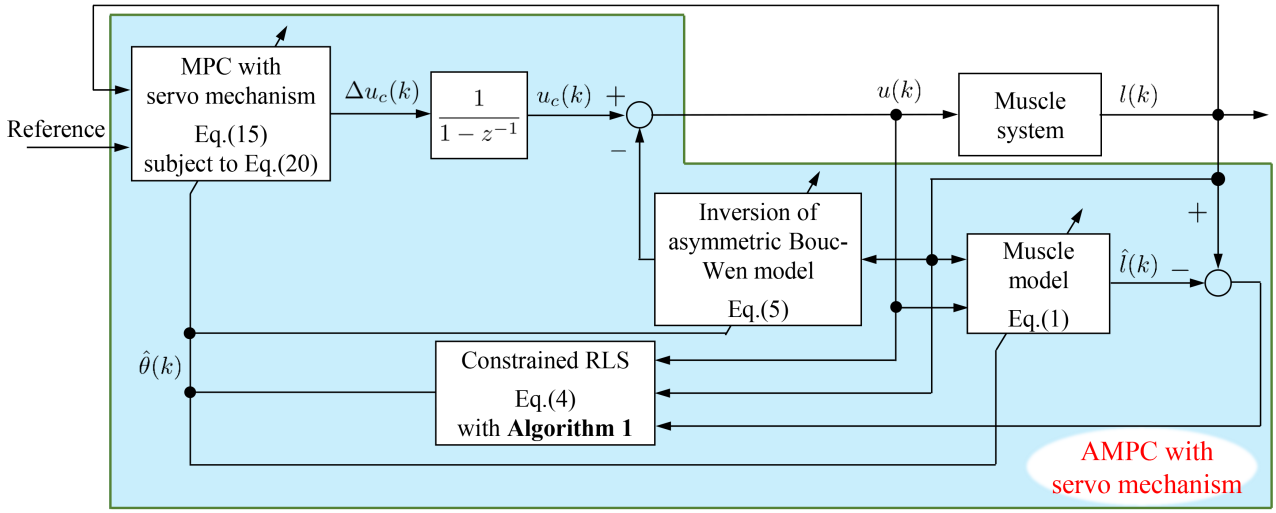

Fig. 6 Schematic block diagram of the AMPC with servo mechanism using inverse of asymmetric Bouc-wen model

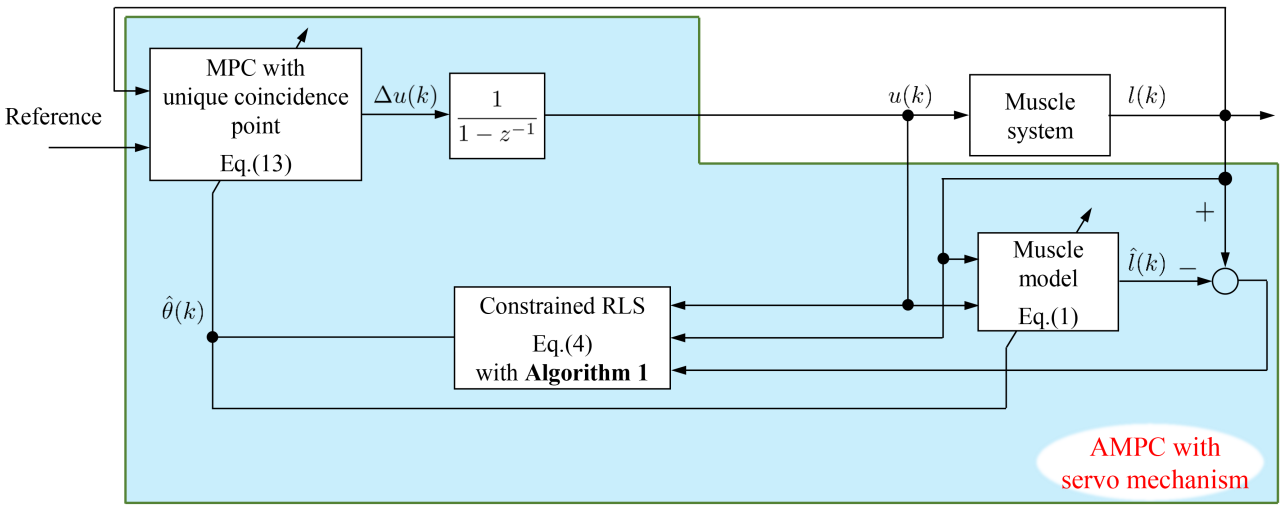

Fig. 7 Schematic block diagram of the AMPC with unique coincidence point

4 Experiment

4.1 Experimental conditions

In this section, we conduct experiment to compare four control methods: MPC with unique coincidence point, MPC with servo mechanism, AMPC with unique coincidence point, and AMPC with servo mechanism. The sampling period is 0.1[s] and a reference is sinusoidal wave with an offset of 35 [mm], amplitude of 30 [mm], and frequency of 0.1[Hz]. Experiments are conducted by circuit in Fig.1 and setup in Fig.2 applying parameters estimated under loads corresponding to 44 [N] and 68 [N]. Tracking control performance in the steady state response from 10 [s] to 40 [s] is evaluated by Eq.(21).

$$\bar{e} = \frac{1}{301}\sum_{k=101}^{401} |r(k) - l(k)| \tag{21}$$

Table 5 Control parameters of each control method for the displacement control

Control parameters	MPC with unique coincidence point	MPC with servo mechanism	AMPC with unique coincidence point	AMPC with servo mechanism
H_p	2	5	2	5
H_u	-	5	-	5
Q	-	{5, 5, 5, 5, 5}	-	{5, 5, 5, 5, 5}
Q_s	-	2	-	2
R	-	15	-	15
$P(0)$	-	-	diag{200 200 200 50 50 50 50 50 50 50 20 20 20 20}	

4.2 Experiments of MPC with unique coincidence point and MPC with servo mechanism

Firstly, we conducted experiments to observe the control performance of MPC with unique coincidence point and MPC with servo mechanism. Note that the experiments utilize fixed predictors, which are obtained by a preliminary identification under 44 [N]. Figures 8 and 9 show experimental results of the tracking control with MPC with unique coincidence point and MPC with servo mechanism under load of 44 [N] and prediction error of predictor in each control method under load of 44 [N] from 10 to 40 [s], respectively. In addition, Figs.10 and 11 show experimental results of these controls for the load of 68 [N] from 10 to 40 [s], respectively.

It is obvious that MPC with servo mechanism has higher control performance than MPC with unique coincidence point from Figs.8 and 10. Table 6 summarizes control performances of each control method under two types of load. As Table 6 shows, MPC with servo mechanism improves control performance more than 0.94 [mm] when compared to MPC with unique coincidence point under both load conditions, even though prediction error is almost same as shown in Figs.9 and 11. These results exhibit that it is valid for the muscle system to take multi coincidence points and to include integrator in evaluation function. Moreover, predictor in MPC with servo mechanism obtained almost same precision whereas its predictor used linear model. This result implies that linearization technique works well for the muscle system. However, we observe that prediction error has bias compared with case of load of 44 [N] as compared Figs.9 to 11. Control performance of MPC with unique coincidence point was degraded by load change, while MPC with servo mechanism maintains its control performance. This result indicates that integrator of MPC with servo mechanism works to eliminate tracking error. Therefore, with aforementioned reason, MPC with servo mechanism is valid for load change of the muscle.

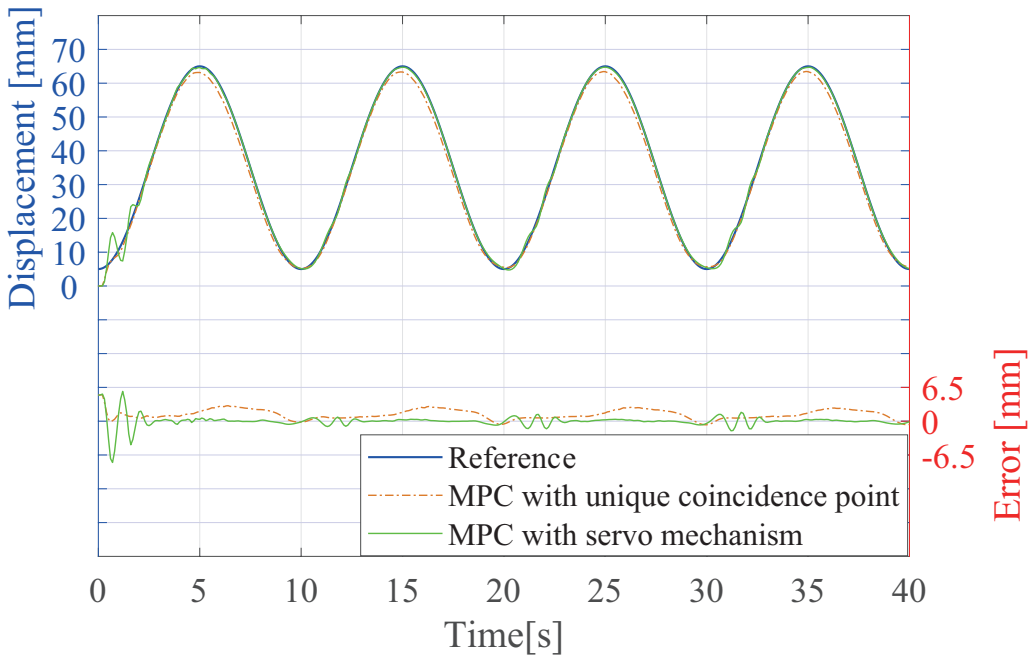

Fig. 8 Tracking performance of MPC with the servo mechanism and MPC with unique coincidence point under the load corresponding to 44 [N]

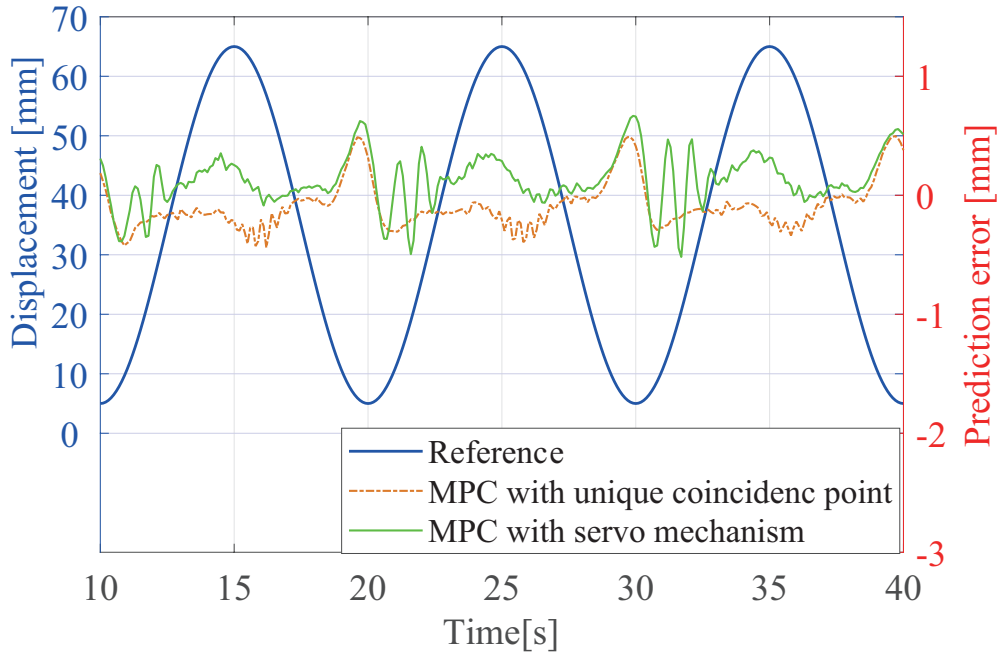

Fig. 9 Prediction error of predictor in MPC with servo mechanism and MPC with unique coincidence point from 10 to 40 [s] under the load corresponding to 44 [N]

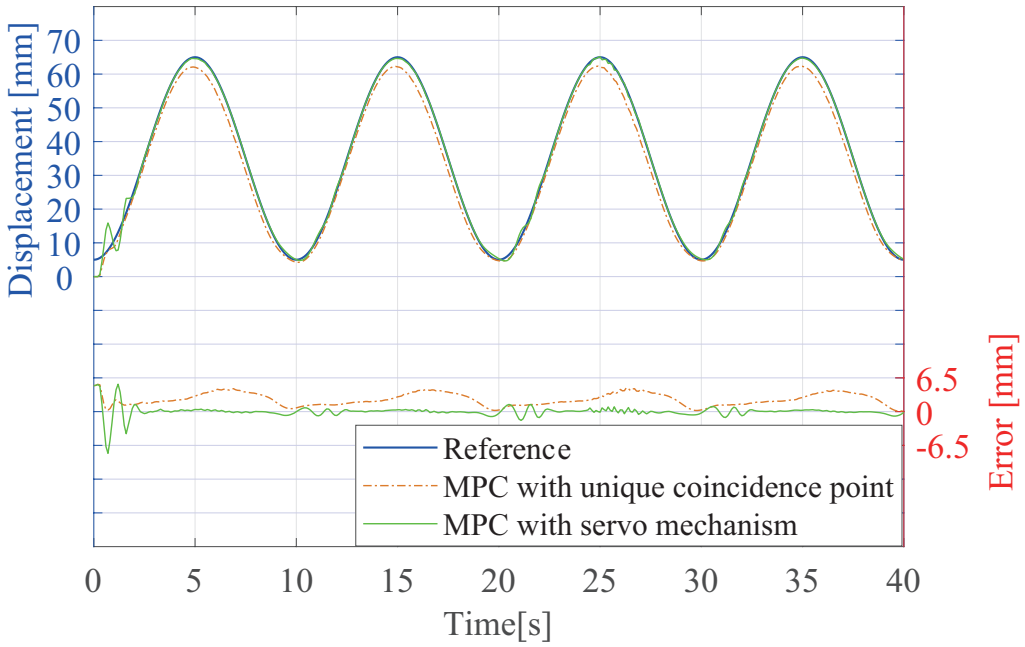

Fig. 10 Tracking performance of MPC with the servo mechanism and MPC with unique coincidence point under load corresponding to 68 [N]

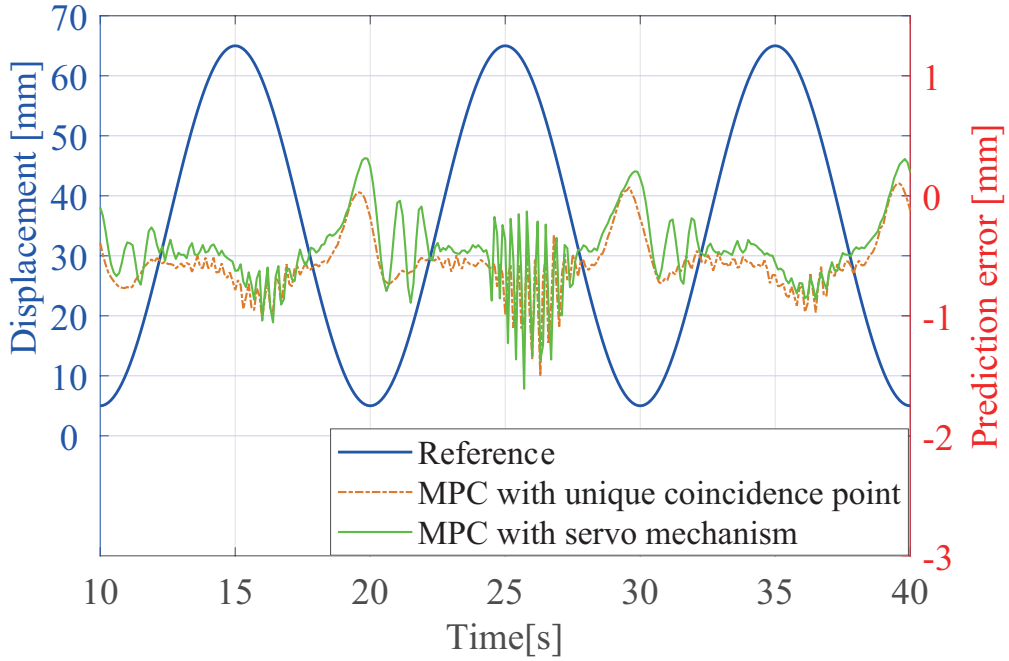

Fig. 11 Prediction error of predictor in MPC with servo mechanism and MPC with unique coincidence point from 10 to 40 [s] under the load corresponding to 68 [N]

Table 6 Control performance comparison of MPC with servo mechanism and MPC with unique coincidence point under loads

Method / Load	MPC with the servo mechanism	MPC with unique coincidence point
44 [N]	0.33 [mm]	1.27 [mm]
68 [N]	0.33 [mm]	2.25 [mm]

4.3 Experiments of the AMPC with unique coincidence point and AMPC with servo mechanism

Next, we conducted experiments to observe control performances of AMPC with unique coincidence point and AMPC with servo mechanism. Note that these experiments introduce constrained RLS algorithm in predictor to compensate parameter error. Figures 12 and 13 show experimental results of the tracking control with AMPC with unique coincidence point and AMPC with servo mechanism under load of 44 [N] and prediction error of predictor in each control method under load of 44 [N] from 10 to 40 [s], respectively. In addition, Figs.14 and 15 show experimental results of these controls for the load of 68 [N] from 10 to 40 [s], respectively.

Table 7 summarizes these control performances and it is clear that AMPC with servo mechanism improves control performance more than 0.79 [mm] when compared to AMPC with unique coincidence point and more than 0.04 [mm] when compared to MPC with servo mechanism. As Table 7 demonstrates, AMPC with unique coincidence point dramatically improves control performance when compared to MPC with unique coincidence point. On the other hand, AMPC with servo mechanism barely improves control performance when compared to MPC with servo mechanism, while prediction error is reduced. From these results, multi coincidence points and integrator give a major effect on control performance under different loaded conditions.

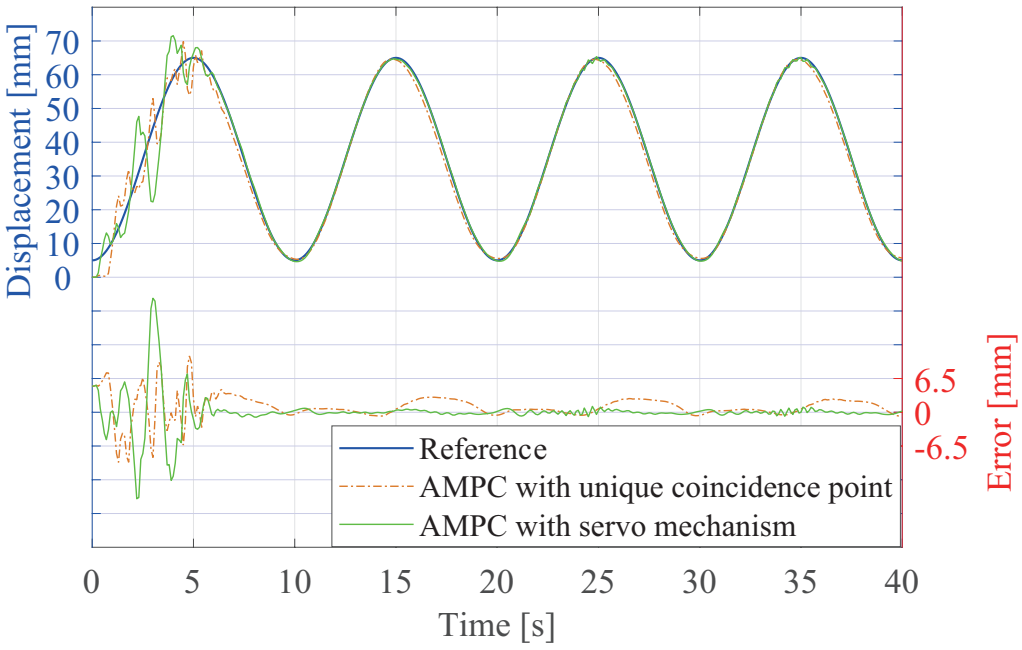

Fig. 12 Tracking performance of AMPC with the servo mechanism and AMPC with unique coincidence point under load corresponding to 44 [N]

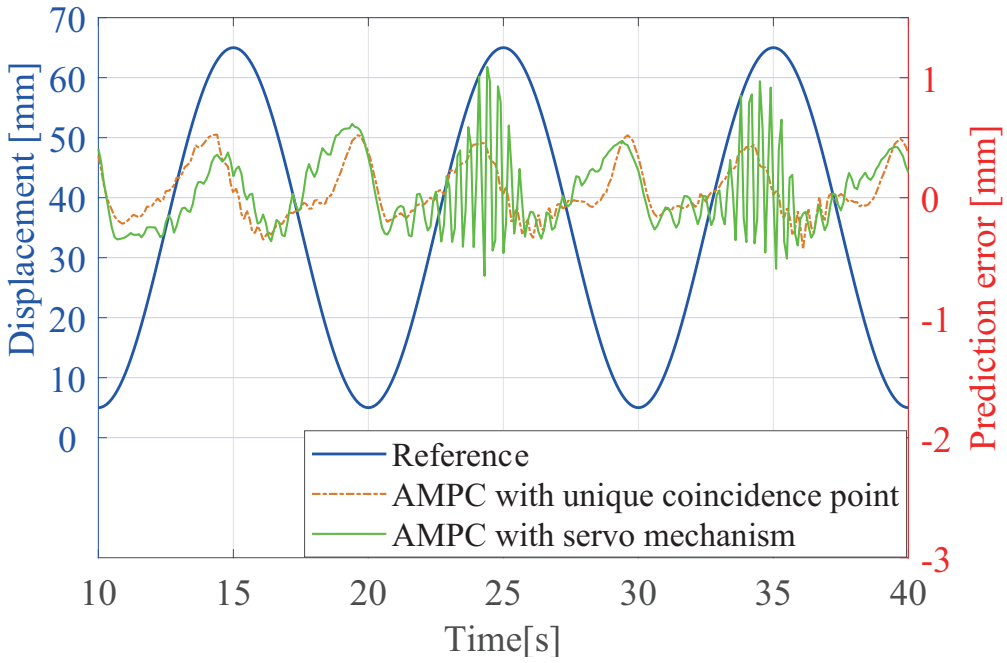

Fig. 13 Prediction error of predictor in AMPC with servo mechanism and AMPC with unique coincidence point from 10 to 40 [s] under the load corresponding to 44 [N]

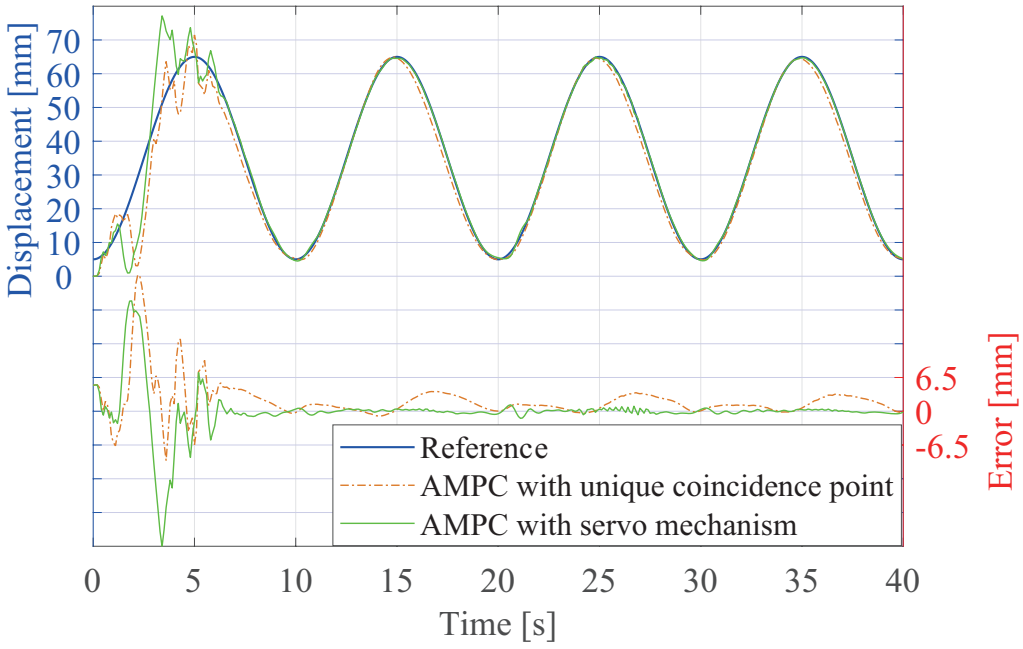

Fig. 14 Tracking performance of AMPC with the servo mechanism and AMPC with unique coincidence point under load corresponding to 68 [N]

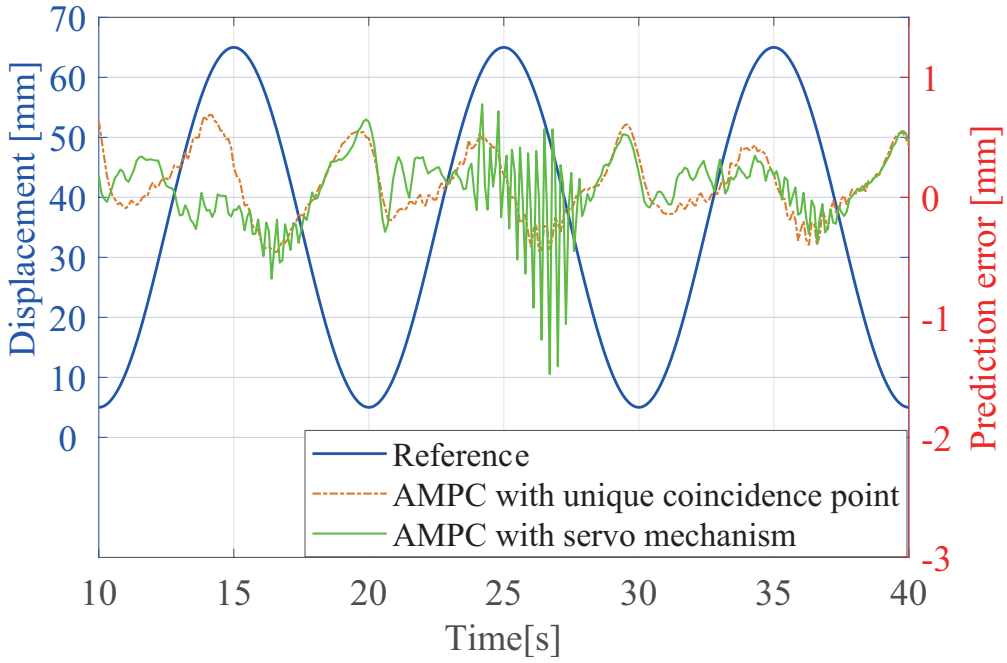

Fig. 15 Prediction error of predictor in AMPC with servo mechanism and AMPC with unique coincidence point from 10 to 40 [s] under the load corresponding to 68 [N]

Table 7 Control performance comparison of AMPC with servo mechanism and AMPC with unique coincidence point under loads

Method / Load	AMPC with the servo mechanism	AMPC with unique coincidence point
44 [N]	0.28 [mm]	1.07 [mm]
68 [N]	0.29 [mm]	1.40 [mm]

4.4 Experiments of the MPC and AMPC with servo mechanism for other reference trajectory

Finally, to show effectiveness of introduction of adaptive algorithm, we conducted experiments to observe control performance of the MPC and AMPC with servo mechanism for different reference. Here, reference is changed to sinusoidal wave with 0.2 [Hz] and same offset/amplitude as in Section 4.1. Re-tuned control parameters are summarized in Table 8.

Note that experimental results show steady state response only from 10 to 40 [s]. Figures 16 and 17 show experimental results of the tracking control with the MPC and AMPC with servo mechanism for changed reference under load of 44 [N] and prediction error of predictor in each control method under load of 44 [N], respectively. In addition, Figs.18 and 19 show experimental results of these controls for the load of 68 [N], respectively.

As Figs.16 and 18 show, the AMPC with servo mechanism reduces tracking error when compared to that of the MPC under each load condition. In addition, Table 9 summarizes control performance of each control method. From the table, we observe that the AMPC with servo mechanism improves control performance more than 0.13 [mm] when compared to that of the MPC under both load conditions. These findings are yielded by reduction of prediction error as compared Figs.17 to 19. The reason why predictor in MPC with servo mechanism yields larger prediction error is that asymmetric Bouc-Wen model cannot characterize the frequency dependent hysteresis of the muscle. In fact, the proposed model has higher error as shown in Fig.20 that shows relationship among 5 steps ahead prediction on the proposed model, re-identified proposed model,

and displacement of muscle when inputted sinusoidal wave with the amplitude of 2.5 [V], bias of 4.5 [V], and frequency of 0.2 [Hz]. Therefore, the experiment results as shown in Figs.8 to 19 indicate that the AMPC with servo mechanism has robustness for not only load change but also frequency change of reference and is effective for the muscle.

Table 8 Control parameters of each control method for the displacement control

Control parameters	MPC with servo mechanism	AMPC with servo mechanism
H_p	5	
H_u	5	
Q	{5, 5, 5, 5, 5}	
Q_s	2	
R	15	
$P(0)$	-	diag{1000 1000 1000 250 250 250 250 250 250 250 150 150 150 150}

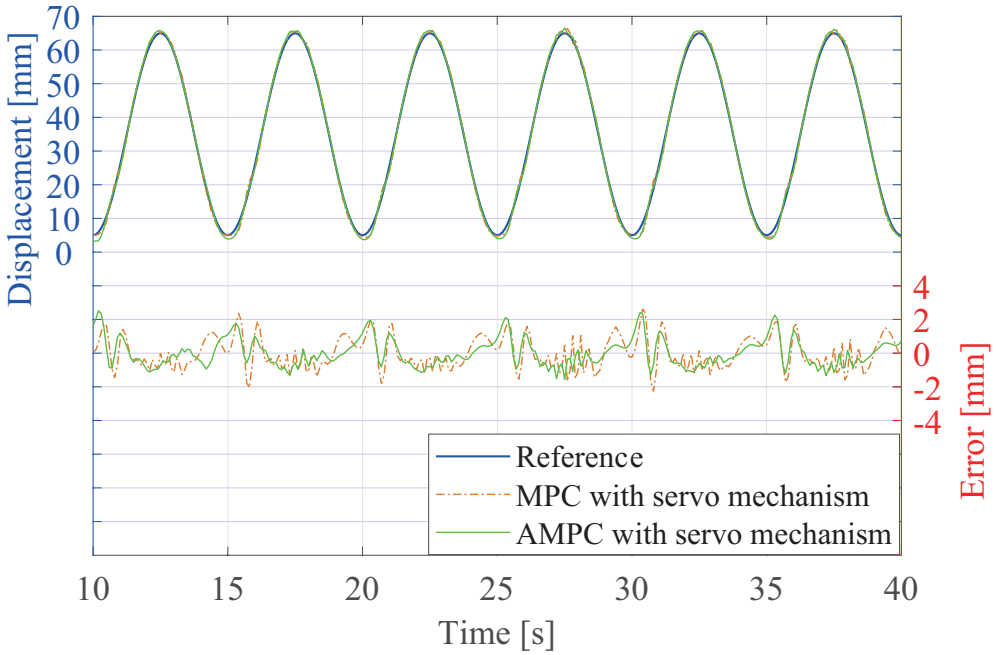

Fig. 16 Tracking performance of MPC and AMPC with the servo mechanism for changed reference from 10 to 40 [s] under load corresponding to 44 [N]

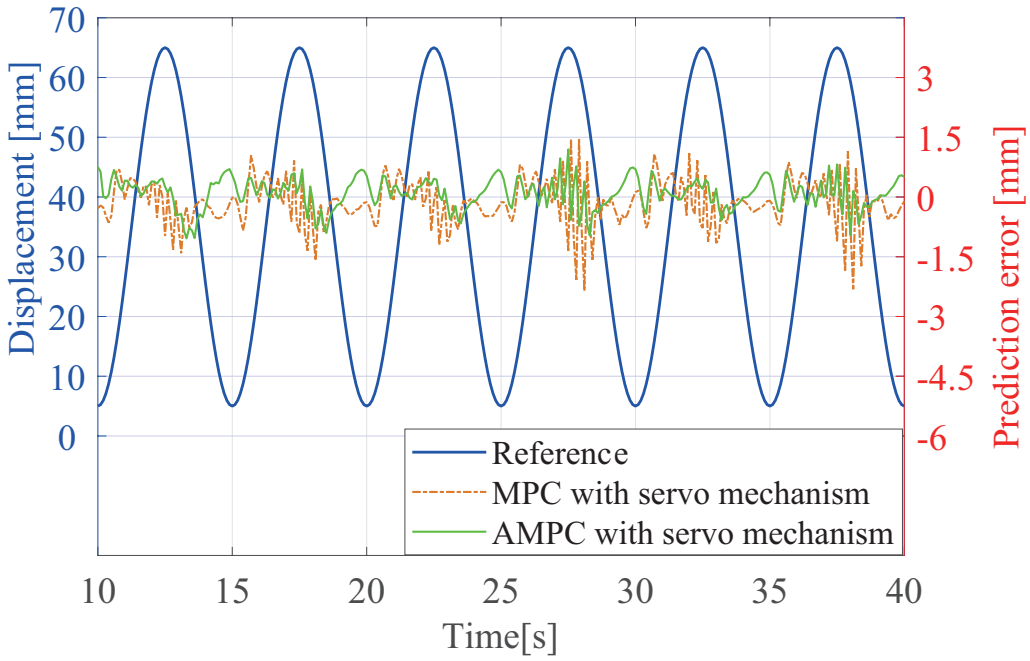

Fig. 17 Prediction error of predictor in MPC and AMPC with servo mechanism from 10 to 40 [s] under the load corresponding to 44 [N]

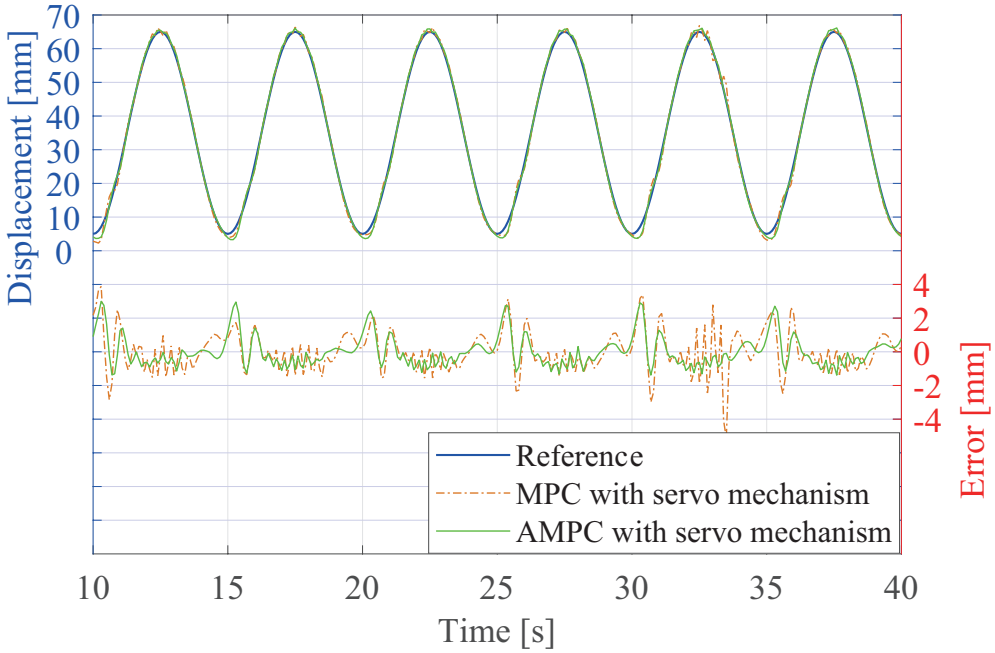

Fig. 18 Tracking performance of MPC and AMPC with the servo mechanism for changed reference from 10 to 40 [s] under load corresponding to 68 [N]

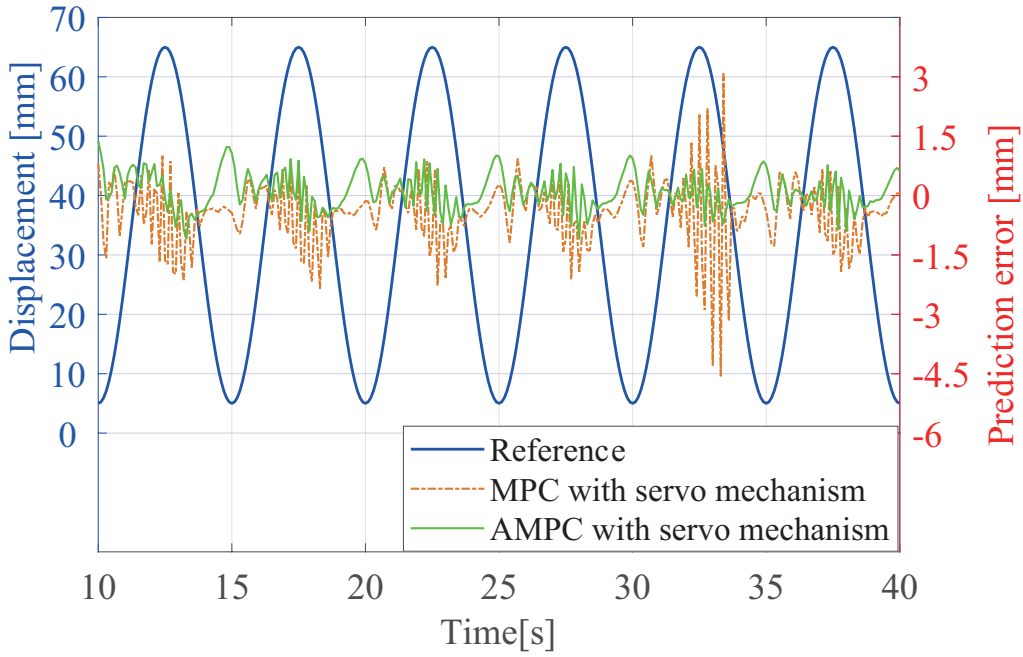

Fig. 19 Prediction error of predictor in MPC and AMPC with servo mechanism from 10 to 40 [s] under the load corresponding to 68 [N]

Table 9 Control performance comparison of MPC and AMPC with servo mechanism for another reference under loads

Method / Load	AMPC with the servo mechanism	MPC with the servo mechanism
44 [N]	0.67 [mm]	0.80 [mm]
68 [N]	0.68 [mm]	0.91 [mm]

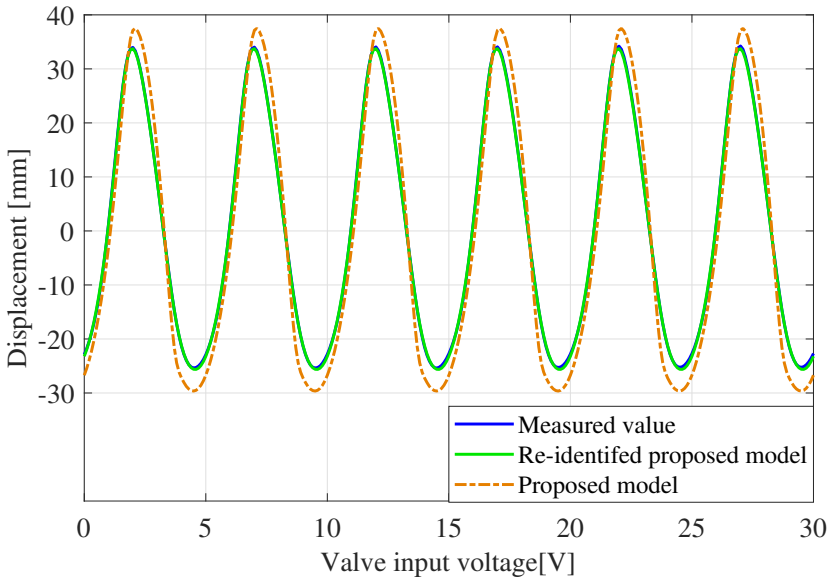

Fig. 20 Comparison of among 5 steps ahead prediction on the proposed model, re-identified proposed model, and displacement of muscle when sinusoidal wave is applied with the amplitude of 2.5 [V], bias of 4.5 [V], and frequency of 0.2 [Hz]

5 Conclusion

This paper discussed modeling and linearization technique based on the asymmetric Bouc-Wen model, and two kinds of controller design for the tap water driven muscle system. The proposed model showed high fitness relative to the measured output and could express asymmetric hysteresis characteristics of the muscle. Subsequently, inverse of the asymmetric Bouc-Wen model was applied to linearize the muscle system. The authors introduced model predictive control with servo mechanism using linearization technique for displacement control of the muscle system. This control method improved control performance more than 0.84 [mm] when compared to model predictive control with unique coincidence point. Additionally, we incorporated constrained recursive least square algorithm to each control method to improve robustness for load changing and to compensate parameter error. As a result, adaptive model predictive control with servo mechanism only improved control performance by 0.05 [mm] when compared to that of model predictive control and adaptive model predictive control with unique coincidence point improved control performance more than 0.79 [mm]. Finally, we changed reference to compare control performance of adaptive model predictive conrol with servo mechanism to model predictive control with servo mechanism. This experiment showed that adaptive model predictive control improved control performance more than 0.13 [mm] when compared to that of model predictive control. From these results, this paper showed that adaptive model predictive control with servo mechanism using linearization technique based on asymmetric Bouc-Wen model achieved higher control performance and obtained robustness for not only load change but also frequency change for reference.

However, we tuned control parameters of MPC by trial and error because relationship between control parameters and closed loop properties is not yet clear. In the future, tuning method for MPC with servo mechanism will be discussed to the muscle system.

References

[1] Georgios A, Georgios N, Stamatis M (2011). A Survey on Applications of Pneumatic Artificial Muscles. In: Proceeding of the 24th, Mediterranean Conference on Control and Automation, pp.1439-1446

[2] Finn C (2005). Trends in Design of Water Hydraulics Motion Control and Open-Ended Solutions. In: Proceeding of the 6th, JFPS International Symposium on Fluid Power, pp.420-431

[3] Shinmpei M (2011). Aqua Drive System: A Technology Using Tap Water and Its Applications. In Proceeding of the 8th, JFPS International Symposium on Fluid Power, pp.26-37

[4] Ahmed S N, *et al.* (1994). Generalized Variable Structure Model Reference Adaptive Control of One-Link Artificial Muscle Manipulator in Two Operating Modes. In: IEEE International Conference on Systems, Man and Cybernetics, pp.1944-1950

[5] Pablo C, Zhong P J, Daniel W (2001). Nonlinear Control of a Pneumatic Muscle Actuator: Backstepping vs. Sliding-mode. Proceedings of 2001 IEEE International Conference on Control Applications, pp.167-172

[6] Aron P A, *et al.* (2010) Modeling in Modelica and Position Control of a 1-DoF Set-up Powered by Pneumatic Muscles. *Mechatronics*, Vol. 20, pp.535-552. doi: 10.1016/j.mechatronics.2010.05.002

[7] Xiangrong S (2010) Nonlinear Model-based Control of Pneumatic Artificial Muscle Servo Systems, *Control Engineering Practice*. Vol. 18, pp.311-317. doi: 10.1016/j.conengprac.2009.11.010

[8] Jun w, *et al.* (2014) Nonlinear Disturbance Observer-Based Dynamic Surface Control for Trajectory Tracking of Pneumatic Muscle System, IEEE Transaction on Control Systems Technology. Vol. 22, pp.440-455. doi: 10.1109/TCST.2013.2262074

[9] Chih J L *et al.* (2015) Hysteresis Modelling and Tracking Control for a Dual Pneumatic Artificial Muscle System using Prandtl-Ishlinskii Model. *Mechatronics*, Vol.28, pp.35-45. doi: 10.1016/j.mechatronics.2015.03.006

[10] Takahiro K, Manabu S (2011) Control of a Parallel Manipulator Driven by Pneumatic Muscle Actuators Based on a Hysteresis Model. *Journal of Environment and Engineering*, Vol. 6, pp.316-327. doi: 10.1299/jee.6.316

[11] Harald A, Dominik S (2014) Comparison of Model-Based Approaches to the Compensation of Hysteresis in the Force Characteristic of Pneumatic Muscles. *IEEE Transactions on Industrial Electronics*, Vol. 61, pp.3620-3629. doi: 10.1109/TIE.2013.2287217

[12] Geng W, Guoqiang C, Fuzhong B (2015) Modeling and Identification of Asymmetric Bouc-Wen Hysteresis for Piezoelectric Actuator via A Novel Differential Evolution Algorithm. *Sensors and Actuators A: Physical*, No. 235, pp.105-118. doi: 10.1109/TIE.2013.2287217

[13] Jan M M (2002) Prediction Control with Constraints, Prentice Hall, p.290

[14] Jacob M, Stephen B (2012) CVXGEN: A Code Generator for Embedded Convex Optimization. *Optimization and Engineering*, Vol. 13, pp.1-27. doi: 10.1007/s11081-011-9176-9

[15] Graham C G, Kwai S S (2009) Adaptive Filtering Prediction and Control, Dover Publications, pp.58-94

[16] Zhu W, Bian L W, Rui X T (2014) Online Parameter Identification of the Asymmetrical Bouc-Wen Model for Piezoelectric Actuators, *Precision Engineering*. Vol. 38, pp.921-927. doi: 10.1016/j.precisioneng.2014.06.002

[17] Takumi T, *et al.* (2015) Model predictive Trajectory Tracking Control for Hydraulic Excavator on Digging Operation, 2015 IEEE Conference on Control Applications, pp.1136-1141